ACS APPLIED MATERIALS & INTERFACES

Research Article

www.acsami.org

Promoting the Selection and Maintenance of Fetal Liver Stem/Progenitor Cell Colonies by Layer-by-Layer Polypeptide Tethered Supported Lipid Bilayer

I-Chi Lee,[†] Yung-Chiang Liu,[†] Hsuan-Ang Tsai,[‡,§] Chia-Ning Shen,[‡] and Ying-Chih Chang*[,‡]

[†]Graduate Institute of Biochemical and Biomedical Engineering, Chang-Gung University, Tao-yuan 333, Taiwan, R.O.C.

[‡]Genomics Research Center, Academia Sinica, Taipei 115, Taiwan, R.O.C.

Supporting Information

ABSTRACT: In this study, we designed and constructed a series of layer-by-layer polypeptide adsorbed supported lipid bilayer (SLB) films as a novel and label-free platform for the isolation and maintenance of rare populated stem cells. In particular, four alternative layers of anionic poly-L-glutamic acid and cationic poly-L-lysine were sequentially deposited on an anionic SLB. We found that the fetal liver stem/progenitor cells from the primary culture were selected and formed colonies on all layer-by-layer polypeptide adsorbed SLB surfaces, regardless of the number of alternative layers and the net charges on those layers. Interestingly, these isolated stem/progenitor cells formed colonies which were maintained for an 8 day observation period. Quartz crystal microbalance with dissipation measurements showed that all SLB-polypeptide films were protein resistant with serum levels significantly lower than those on the polypeptide multilayer films without an underlying SLB. We suggest the fluidic SLB promotes selective binding while minimizing the cell−surface interaction due to its nonfouling nature, thus limiting stem cell colonies from spreading.

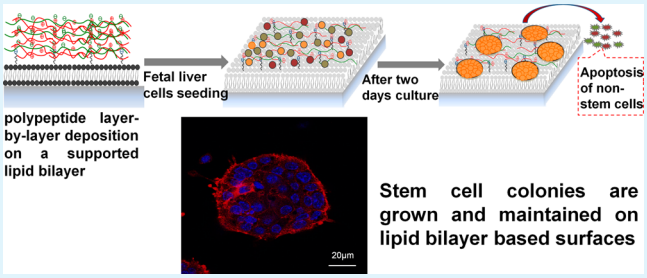

KEYWORDS: *label free, supported lipid bilayer (SLB), layer-by-layer polypeptide films, fetal liver stem/progenitor cells, rare cell isolation, stem cell maintenance*

INTRODUCTION

There is a strong incentive to purify, enrich, maintain, and facilitate production of a large quantity of stem cells for a wide variety of biological and medical applications. It is known that the microenvironment interactions, such as chemical stimulant induced by soluble signaling molecules, electric fields, and mechanical force mediated through integrin-mediated cell−matrix and cell−cell interactions,[1−4] are critical for the stem cell fate. Previously, selective culturing, flow cytometric sorting, and magnetic-activated cell sorting[5−8] have been applied as the first step to isolate the stem cells from primary cells. These affinity-based methods require well-defined biomarkers to isolate scarce stem cells from the entire population and are unusable when a target cell lacks effective biomarkers. Therefore, it is considered that variation of the physical microenvironment could regulate stem cell behaviors and may offer opportunities for stem cell selection that does not require biomarkers.

Surface properties, such as surface charges, hydrophilicity, protein surface modification, and surface roughness, have been evaluated for their effects on cell adhesion and stem cell behavior via integrin mediated interactions.[9,10] A layer-by-layer technique for making polyelectrolyte multilayer (PEM) films[11] offered a simple method to prepare highly tunable thin films and versatile tools to form a series of surfaces with adjustable properties. It has been shown that, by varying the electrolytes or process conditions,[12−16] the properties of the films, including thickness, rigidity, chemical composition, hydrophilicity, and surface charges, could be altered at will.[17−19] Among the PEM films that have been used, recent studies have used PEM films composed of the synthetic polypeptides poly(L-lysine) (PLL) and poly(L-glutamic acid) (PLGA) to explore the effects of film properties on cells.[20,21] We have used PLL/PLGA PEM films to successfully identify the optimal conditions for selecting and maintaining fetal mouse liver stem/progenitor cells (FLSPCs) colonies.[22,23] Specifically, it was found that the FLSPCs form colonies and are maintained on those thick films, while adhesive cells such as fibroblast and hepatocytes tend to be adhesive and spread on thinner, rigid PEM films. For a prolonged period of culture up to 8 days, the FLSPCs colonies maintain small colonies on the thick films, while the majority of FLSPCs differentiated and spread on the thin films. With further investigation on the surface properties of these films, it was discovered that thick films that promote the FLSPCs colony formation and maintenance are more hydrated, elastic, and protein resistant than those thin films, while chemical

Received: June 19, 2014
Accepted: September 22, 2014
Published: September 22, 2014

compositions and surface charges had little influence on thick films in the PEM system.

It is well recognized that cell morphology and functions strongly depend on substrate stiffness under conditions where chemical signals are constant.[24,25] A previous study using fibroblast cells showed that cells displayed a flatter morphology and stable adhesion on a stiff substrate.[26] In contrast, numerous culture systems have been developed to promote cell−cell contact and culture cells in aggregate structures by using soft materials to maintain an undifferentiated phenotype of stem cells or regulate proper molecular signaling.[27−29] Therefore, it is considered that the hydrated elastic films are cell and protein resistant; in contrast, the rigid films promote adhesion because the proteins are prone to adsorb on them. Herein, we would like to construct a protein resistant film independent of surface rigidity, surface charges, chemical composition, and physical properties to characterize stem cell behavior in depth.

Because the correlation of a given protein with cells cannot be evaluated when the protein is adsorbed on a surface in an uncontrolled manner, there is a need to provide a protein resistant, "non-fouling" platform that can be used to immobilize specific recognition ligands or ligand-free materials inert to nonspecific adsorption. Nonfouling surfaces that resist nonspecific adsorption of proteins, bacteria, and higher organisms are of particular interest with diverse applications ranging from marine coatings to diagnostic devices or biomedical implants.[30−33] Researchers have developed many biomaterials that resist protein adsorption.[34−39] Previous research has shown that supported lipid bilayers (SLBs) are a good nonfouling material with unique properties close to the cell membrane, such as lateral diffusion and the ability to control the spatial location of ligands.[40−43]

In this study, a label-free biomimetic system, composed of PEM films adsorbed on SLBs, was established to select and maintain FLSPCs colonies and to study the effect of surface properties on stem cell maintenance without protein interference. The SLB-PEM system provides a series of substrates with surface properties variation to model the stem cell−materials interaction. In addition, the SLB-PEM system can be comprehensively compared with our previous PEM system that did not include SLBs to determine the effect of the SLBs.[22] FLSPCs colony formation and maintenance ratios were evaluated, and the stem cell markers of the colonies were identified by immunostaining. The films' conjugations and their interactions with serum proteins were characterized by quartz crystal microbalance with dissipation monitoring (QCM-D). In the serum-containing medium, the colony−materials interaction and adhesive evaluation were measured with a vinculin test.

EXPERIMENTAL SECTION

Preparation of SLB. All chemicals were obtained from commercial sources and used without further purification. Water was deionized and purified using a Milli-Q unit (Milli-Q plus, Millipore, France). The preparation of vesicles doped with *N*-glutaryl phosphatidyl ethanolamine (NGPE) vesicles and formation of SLBs follow the procedures described in our previous work.[44] In brief, 10% of NGPE (Avanti Polar Lipids, Alabaster, AL, U.S.A.) by weight was mixed with 1-palmitoyl-2-oleoyl-*sn*-glycero-3-phosphocholine (POPC, Avanti Polar Lipids), dissolved in chloroform (total mass was 5 mg), and then dried under a gentle stream of nitrogen to form a thin lipid film on the wall of a tube. Next, the tube was placed in a vacuum for 3 h. The thin lipid film was subsequently resolved in 1.0 mL of pH 5.5 Tris buffer solution with 10 mM Tris and 100 mM NaCl forming a vesicle solution. The vesicle solution was then extruded through a 100 nm filter (Avanti Polar Lipids) and then through a 30 nm filter (Avanti Polar Lipids). Subsequently, the vesicle solution was transferred to a hydrophilic glass, which was treated with oxygen plasma (contact angle <5°), for the cell culture to form a SLB.

Preparation of PEM Films on SLB. The preparation of polypeptide films adsorbed on the SLB by electric charge interaction followed the procedure as described in the literature with some modifications.[9] Physical deposition of layer-by-layer polypeptide films was performed by batch under static conditions as follows: (1) dissolving all polypeptides in 10 mM Tris-HCl buffer with 0.15 M NaCl, pH 7.4; (2) immersing SLB substrates in PLL (MW: 15 000−30 000; Sigma, St Louis, MO) solution (1 mg/mL) for 10 min at room temperature, followed by rinsing the SLB-PLL substrates with 1 mL of Tris-HCl buffer for 1 min; (3) to couple PLGA to the SLB-PLL substrates, immersing the SLB-PLL substrates in PLGA solution (MW: 3000−15 000, Sigma, St Louis, MO, 1 mg/mL) for 10 min, followed by rinsing the substrates with 1 mL of Tris-HCl buffer for 1 min; and (4) cleaning the substrates with fresh phosphate-buffered saline (PBS) solution to remove uncoupled polypeptides. The above steps were repeated to obtain an SLB-$(PLL/PLGA)_n$ substrate, where n denotes the number of polyelectrolyte pairs generated by repeating the above steps, wherein n = 0.5 denotes half a polyelectrolyte pair, PLL only, and n = 1 denotes a complete polyelectrolyte pair, PLL and PLGA.

Isolation of FLSPCs and Formation of FLSPCs Colonies. All animal experiments that used mice were approved by the Academia Sinica Institutional Animal Care and the Chang Gung University Institutional Animal Care Utilization Committees. Single cell suspensions of liver cells were prepared from ED13.5 embryos of CD1 mice (BioLASCO, Taipei, Taiwan). Mice fetal liver tissue served as the source of FLSPCs. Livers were cut into small pieces and digested at 37 °C in Hanks' balanced salt solution (Gibco, Invitrogen, Gaithersburg, MD) containing 2.5 mg/mL collagenase B (Roche, Basel, Switzerland), 2.4 U/mL Dispase (Invitrogen, Grand island, NY), 2.5 mM $CaCl_2$ (Sigma, St Louis, MO), and 2% heat-inactive fetal bovine serum (Hyclone, Logan, UT). After digestion, liver tissue was dissociated by gentle mechanical pipetting, using wash buffer 3 times, and collected by centrifugation at 500 rpm for 3 min. Fetal liver cell suspensions were resuspended in DMEM/F12 medium (Invitrogen, Grand Island, NY) containing 10% heat-inactive fetal bovine serum, 1× insulin/transferring/selenium (ITS) (Invitrogen, Grand island, NY), 10 mM nicotinamide (Sigma, St. Louis, MO), 20 g/mL gentamicin, and 10 nM dexamethasone and were then seeded on glass coverslips coated with SLB-PEM films.

Quartz Crystal Microbalance with Dissipation Monitoring (QCM-D) Measurements of SLB-PEM Films. The silicon oxide (SiO_2) QCM crystal chips (AT-cut quartz crystals, f_0 = 5 MHz) (Q-Sense AB, Gotebrog, Sweden) were cleaned in 10 mM sodium dodecyl sulfate (SDS), followed by rinsing with Milli-Q water, drying with nitrogen, and exposing to oxygen plasma. Liquids were exchanged by a noncontinuous plug flow, first passing through a temperature controlled loop that was stabilized to 25 °C. All measurements were recorded at the third overtone (15 MHz), and the data was normalized to fundamental frequency (5 MHz) by dividing the data by the overtone number.

Atomic Force Microscopy (AFM) Imaging. AFM experiments were carried out on an atomic force microscope (Asylum Research, Santa Barbara, CA) operated in tapping mode. Microcantilevers from Biolever (Olympus, Tokyo, Japan) were used for all measurements. All measurements were performed in Tris buffer including 150 mM NaCl, 10 mM Tris, and 1 mM EDTA, at pH 7.5. Samples were maintained in a closed fluidic cell. Igor Prosoftware (Wave Metrics, Lake Oswego, OR) was used for image flattening and data analysis of the TM-AFM images.

Fluorescence Recovery after Photobleaching (FRAP) Measurements. To obtain the fluorescence images and monitor the mobility of SLB before and after PEM deposition, Texas Red-DHPE (0.5%, w/w) was incorporated as a tracer into the POPC/NGPE vesicles. Fluorescence measurements were performed with a Leica

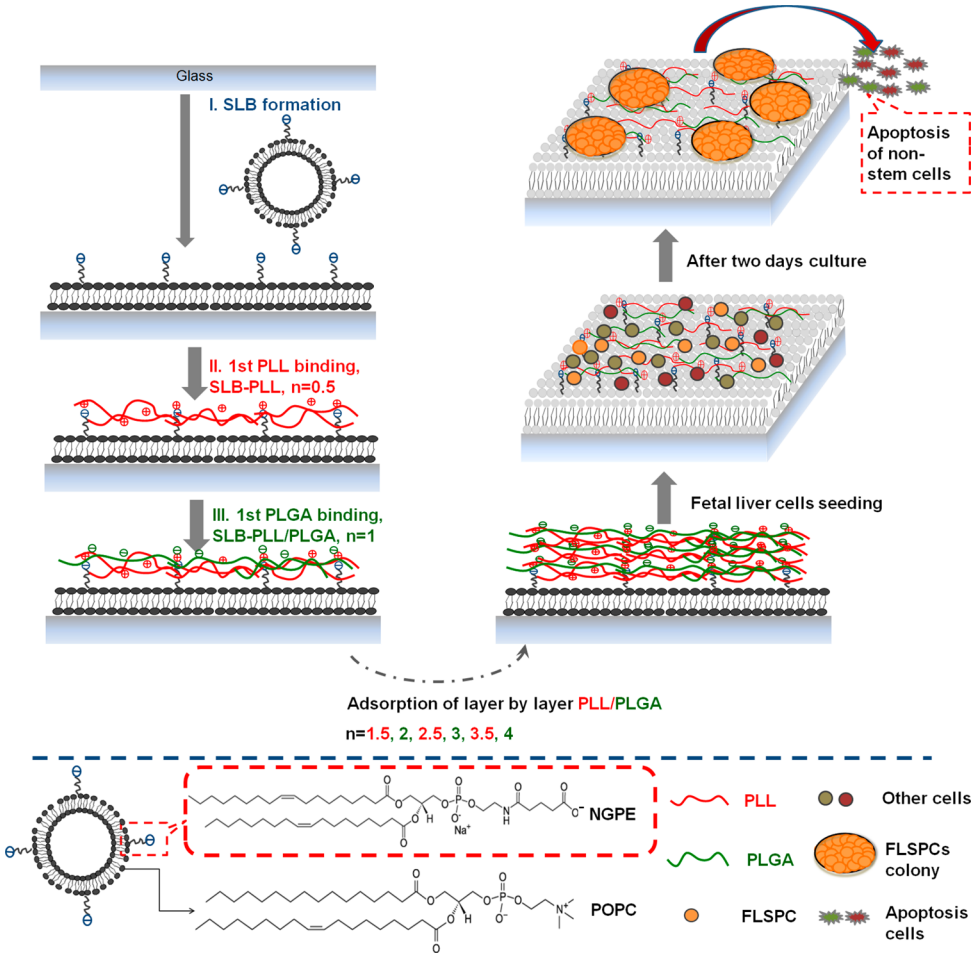

Figure 1. Schematic illustrations (not to scale) of layer-by-layer polypeptides adsorbed on the SLB, fetal cells seeding, and FLSPCs selection. The chemical structure of POPC and NGPE are shown on the bottom. Steps I–III match to the points labeled correspondingly in Figure 2. The SLB-based surfaces were nonfouling, resistant to both serum protein adsorption and nonspecific cells attachment. FLSPCs semiattached on the surfaces and formed colonies but did not differentiate after 8 days.

Spectral Confocal and Multiphoton microscope (Wetzlar, Germany) using the 561 nm line as the source for both bleaching and monitoring fluorescence recovery. The diameter of the bleached spot was 15 μm, and the bleaching time was about 30 s. The data were analyzed by Metamorph software. The diffusion coefficient, D, was related to the half-life of this recovery: $D = r^2/4\tau$, where r is the radius of the bleached spot and τ is the time for half recovery of the fractional integrated fluorescent intensity.

Analysis of the Film Growth and Serum Adsorption Amount. The SLB-polypeptide films buildup process and its subsequent contact with serum were determined with QCM-D. The QCM-D device has the capacity of simultaneously measuring the resonant frequency shift (Δf) and the change in energy dissipation (ΔD). Adsorption of a small mass (Δm) onto the crystal results in a decrease in the resonant frequency (Δf). Given that the mass adsorbed by the crystal is much smaller than the mass of the crystal, the friction between the adsorbed mass and the crystal is negligible. The frequency change of Δf is directly proportional to the adsorbed mass, Δm, according to the Sauerbrey equation $\Delta m = -(\Delta f/(nC))$, where C is the mass-sensitivity constant (5.72m^2 Hz mg^{-1} at f_0 = 5 MHz) and n is the overtone number. The serum adsorption amounts were fitted and determined with the Voigt model in Q-tool software.

Quantification of Colony Numbers, Maintenance Ratio, and Cluster Size Distribution. Single cells suspensions isolated from fetal liver tissue were seeded onto a series of PEM films with and without conjugated SLB films. Colony numbers and maintenance ratios were counted after 2, 4, 6, and 8 days of incubation at 37 °C and 5% CO_2. Populations of cluster size on SLB-PEM films after 2 and 8 days of culture were also determined. Data were analyzed by using Imaging Software-ImageJ for analysis.

Immunofluorescent Staining of FLPSCs Colonies. After 6 days of culture, cells were fixed in chilled (0 °C) 4% paraformaldehyde in PBS for 30 min at room temperature and permeabilized at room temperature in 0.1% Triton X-100 for 30 min. After treating with 2% Roche blocking reagent, the cells were incubated with a primary antibody overnight at 4 °C and then with a secondary antibody for 1 h at room temperature. The primary antibodies were used at the following dilutions: DLK-1 (Santa Cruz Biotechnology) at 1:100 dilution, α-fetoprotein (DakoCytomation) at 1:100 dilution, cytokeratin 19 (DakoCytomation) at 1:100 dilution, cytokeratin 7 (Novocastra) at 1:100 dilution, and vinculin (Sigma) at 1:300 dilution. The secondary antibodies were used at the following dilutions: fluorescein antirabbit IgG (H + L) (1/300; Vector Laboratories), fluorescein antimouse IgG (H + L) (1/300; Vector Laboratories), and fluorescein antigoat IgG (H + L) (1/300; Vector Laboratories). Cell nuclei were stained with 4′,6-diamidino-2-phenylindole (DAPI, Vector Laboratories) at 1:10 000 dilution. Immunostained specimens were viewed with a SPOT camera mounted on a Zeiss Axioplan 2 microscope.

RESULTS

The procedure of layer-by-layer polypeptides adsorbed on the SLB is illustrated in Figure 1. The formation of PEM films was through the electrostatic interaction of PLL as a polycation and PLGA as a polyanion. Steps (I–III) shown in the process

schematic in Figure 1 correspond to the process steps shown in the QCM-D response in Figure 2A. After formation of the SLB-PEM structure, FLSPCs were seeded and cultured on the composite structure.

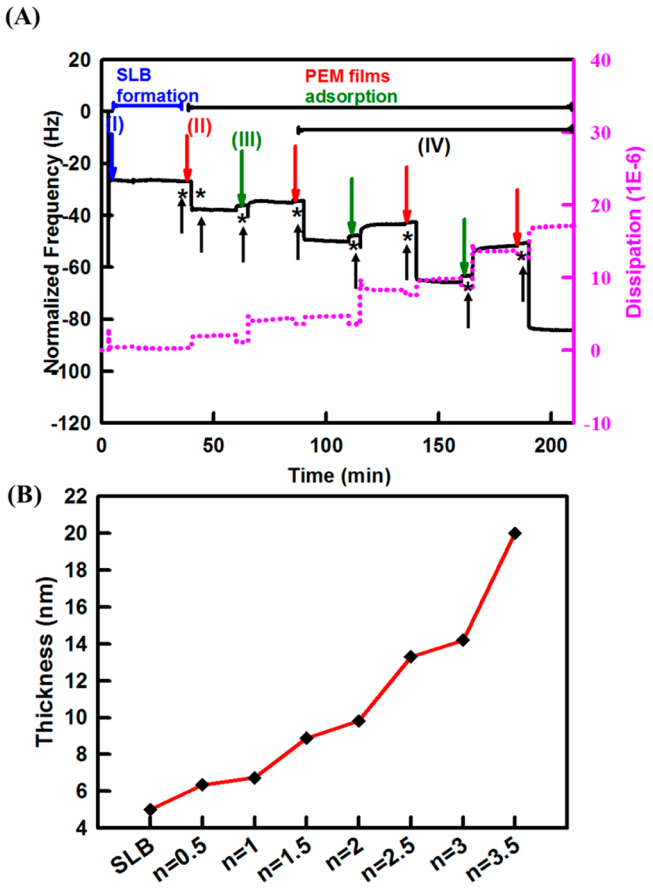

Figure 2. (A) Kinetics of the buildup of the layer-by-layer polypeptides adsorbed on the SLB, monitored by QCM-D. Lipid vesicles (POPC/NGPE 10%) were introduced at point (I), followed as adsorbed and ruptured to form a SLB on the SiO_2 surface. PLL solution was injected into the QCM-D chamber at point (II) and adsorbed on SLB with a charge−charge interaction, followed by PLGA solution flowed in at point (III) and layer-by-layer adsorption to form polypeptide films adsorbed on SLB. Extensive rinsing with pH 7.2 Tris buffer, denoted as ∗, was perform after each step. The black and pink lines represent the response curves of normalized frequency and dissipation, respectively. (B) Model-fitted values for layer thickness using the Sauerbrey equation and Voigt-based model.

SLB Formation, SLB-PEM Conjugation, and Film Growth. Extruded POPC vesicles doped with 10% NGPE lipids formed high quality SLBs on SiO_2. The quality of the bilayers was assessed from Δf and ΔD profiles. Figure 2A shows the QCM-D profile of bilayer formation and illustrates the characteristic two-stage process. Figure 2B shows the model fitted values for layer thickness using the Sauerbrey equation and the Voigt-based model. The QCM-D response can be used to view the development of the SLB-PEM conjugate as outlined in Figure 1. Initially, the SLB was formed. Approximately 2.5 min after the start, intact vesicles adsorbed onto the surface of a hydrophilic substrate, as indicated by the rapid drop in Δf and the increase in ΔD (increased dissipative energy loss in the film). The total mass originated from the sum of lipid mass and trapped water. Second, at a critical point at 3 min, the vesicles ruptured to form a planar bilayer. Δf then increased because of the release of water from rupturing and fusing vesicles. The increase in Δf was accompanied by a decrease in ΔD, signaling transformation into a more rigid film. Once the bilayer formation was complete (at 4 min), neither the Δf signal nor the ΔD signal was affected by the buffer rinse (from 31 to 40 min, denoted as ∗).

After the SLB formation, the layer-by-layer PEM films were built up on the SLB. The construction of the SLB-PEM substrate started with PLL adsorption on the SLB substrate at point (II), forming a physically adsorbed PLL film (SLB-PLL), followed by PLGA adsorption forming a SLB-$(PLL/PLGA)_1$ substrate at point (III). When the polyelectrolyte was introduced to the SLB substrate (at 40 min), the decrease in Δf and the increase in ΔD implied the formation of a new layer on the SLB substrate. The final substrate, the SLB-$(PLL/PLGA)_4$ substrate, measured approximately −78 Hz in Δf and 0.14 in ΔD, which are comparable with our previous results on the PEM-only system.[44] In comparison to the PEM-only substrates, the increase in Δf of the SLB-PEM substrate was lower and the thickness was thinner. Figure 2B showed that the thickness of the SLB-$(PLL/PLGA)_{3.5}$ substrate was 20−25 nm. Both PEM and SLB-PLM systems observed an increase in the mass and thickness of PLL/PLGA for up to four layers. In the SLB-PEM system, where SLB was the first layer, substantially less polyelectrolyte was adsorbed compared to the PEM-only system as indicated by the smaller change of frequency upon deposition.

The dissipation factor (D) indicates the energy losses in the system and contains information about film interaction with the bulk solutions. Previous literature has revealed that the adsorption/desorption, as well as structural changes, and the viscoelastic properties of the adsorbed multilayer may affect the variation of dissipation and may provide the mechanical/structural properties of the substrate.[45] In general, rigid structures have a minimal effect on dissipation. In contrast, thick and flexible structures dissipate a lot of energy. Hence, the dissipation can be seen as a measure of the rigidity or viscoelasticity of the adsorbed film. In the SLB-PEM system, the increase in ΔD when a PLGA layer was added was greater than the increase in ΔD when a PLL layer was added. This indicates that the PLGA layer is more flexible than the PLL layer. In addition, Figure 2A shows that the dissipation variation upon the SLB formation section was small, indicating that the SLB was a rigid substrate. The dissipation variation of SLB-PEM (n = 3.5) was about 15.4; that is equally rigid with PEM (n = 1.5). It is revealed that the SLB-PEM system is more rigid and the rigidity variation is smaller than that of the PEM system. It is reasonable to suggest that the maintenance ratio of the stem cell colony regardless of its rigidity in this system.

Furthermore, the fluidity and the coverage of lipid layers were investigated to confirm SLB quality. AFM was also used to examine the surface morphology of SLB-PEM films on mica. A small defect of the lipid layer on the mica surface was imaged, permitting us to check the thickness of the lipid layer, which was consistent of the QCM-D data of ∼4 nm for a typical SLB (Figure S1-A, Supporting Information). As shown in Figure S1-B,-C, Supporting Information, polypeptide fibrils formed on top of the lipid bilayer surface, forming heterogeneous domains where the roughness was increased with the number of deposited polypeptide layers. Our previous study has also revealed that the surface morphology with some aggregated

surface pattern and the roughness were observed to increase as the layer of the PEM film increased.[46]

Lateral lipid diffusivity in the SLB-PEM films was further evaluated by FRAP. For SLB without PEM, recovery was fast and relatively complete (Figure S2-A, Supporting Information). Although the relative diffusion coefficient was decreased from 1.135 to 0.709 as the films varied from SLB to SLB-$(PLL/PLGA)_5$, the lipid mobility after the PEM deposition (Figure S2-B, Supporting Information) was confirmed.

Formation of Colonies of FLSPCs on SLB-PEM Substrates. The phase contrast images of FLSPCs seeded on PEM substrates and PEM adsorbed on SLB substrates after 8 days of culture are shown in Figure 3A,B, respectively. Schematic representations of colony morphologies on each surface are illustrated above the corresponding phase contrast image. Even though colony formations were present on all of the substrates, only on the PLL, SLB, and SLB-PLL substrates did the morphology of the cell colonies change noticeably after 8 days of culture, as shown in Figure 3A-a,A-b,B-a, respectively. The change in colony morphology shows that the FLSPCs migrated and spontaneously differentiated into functional cells on those substrates. In contrast, the colonies' morphologies on the substrates having a higher number of PEM film layers or SLB-PEM were well maintained even after 8 days of culture. In comparison with our previous study,[22] the SLB-based substrates showed the terminal layer had no effect on colony formation. Regardless of the terminal layer being a PLL layer or a PLGA layer, the FLSPC's colony formation was not affected. On the basis of the initial cell seeding density of 1×10^6, the average size of the semiattached cell colonies was estimated to be 30−50 μm after 2 days of culture. On average, 1×10^6 FLSPC cell seeding generated approximately 400 colonies after 2 days of culture on all of the SLB-PEM substrates.

Quantification of Colonies Number and Maintenance Ratio. The number of colonies and maintenance ratios of FLSPCs on 2, 4, 6, and 8 days of culture on a series of substrates, including PEM-treated and SLB-PEM-treated substrates, are shown in Figure 4. The number of colony formations after 2 days of culture depended on the terminal layer when PEM was not conjugated with SLB, with PLGA-terminated PEMs having significantly more colonies than PLL-terminated PEMs. In contrast, we could generate 400 colonies on all SLB-PEM substrates after 2 days of culture, independent of the number of layers in the PEM or the terminal layer. Figure 4A shows the colony number decreased by approximately 50% after 4 days of culture and was at ~12% of its 2 day value after 8 days of culture on the SLB-only substrate. Furthermore, the colony numbers decreased after 4 and 8 days of culture due to spontaneous differentiation especially on SLB-only and low layer number SLB-PEM films. The maintenance ratio equaled the number of colonies after 8 days of culture divided by the number of colonies after 2 days of culture and is shown in Figure 4B. It is revealed that the maintenance ability of the SLB-PEM substrates improved as the number of layers increased, with the best maintenance ratio, effectively 100%, observed for the SLB-$(PLL/PLGA)_4$ substrate.

The results presented in Figure 4 demonstrate that SLB-PEM conjugates provide a better microenvironment, when compared to PEM films without conjugated SLB, for the selection and maintenance of FLSPCs colonies. In our previous research,[22] we showed that, for FLSPCs on a PLL-coated substrate, the colony number was only 200 after 2 days of culture, and the maintenance ratio dropped to 5% after 8 days of culture. The use of an SLB-PLL substrate in the present study doubled the colony formation, forming ~400 colonies after 2 days of culture, and the maintenance ratio increased to 50% after 8 days of culture. Furthermore, the best maintenance ratio in our previous PEM-only system was no more than 50%, whereas all of the maintenance ratios were >50% with the SLB-PEM system.

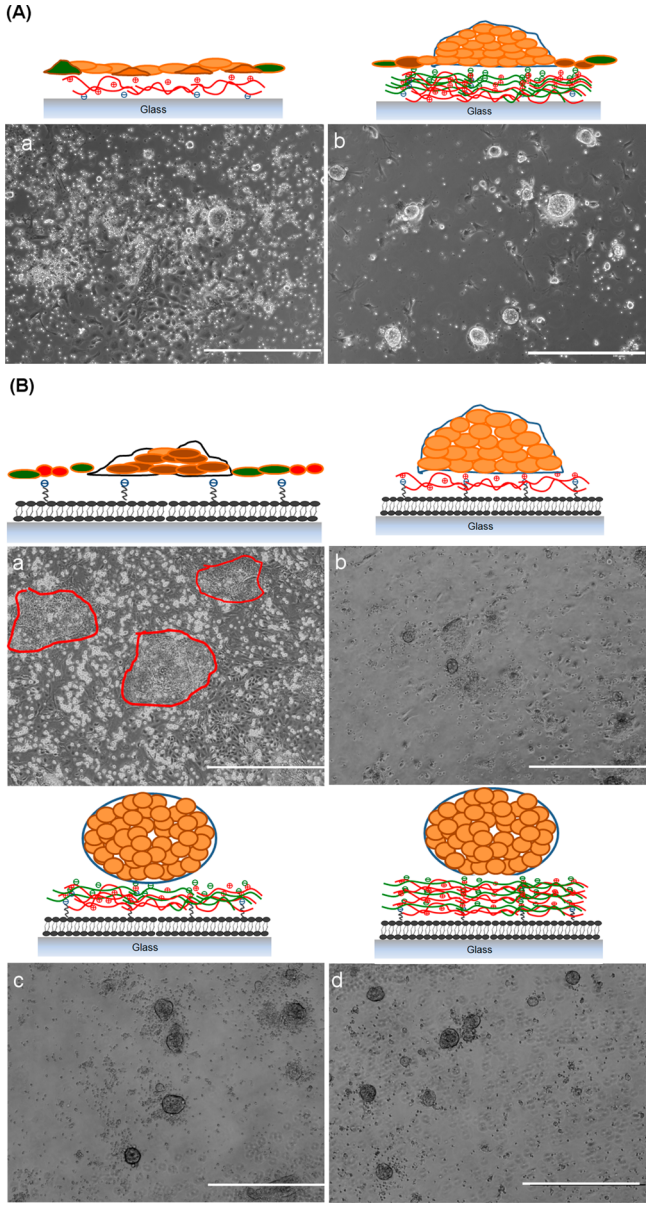

Figure 3. Phase contrast images of fetal liver cells after 8 days of culture after seeding on (A) PLL and PEM substrates without a conjugated SLB and (B) substrates with PLL and PEM adsorbed on SLB. Schematic representations of colony morphologies on each surface are illustrated at the above of images. The red circle lines in (B-a) mark the boundary of the spreading clusters. (A-a) PLL. (A-b) $(PLL/PLGA)_3$ (B-a) SLB. (B-b) SLB-PLL. (B-c) SLB-$(PLL/PLGA)_2$. (B-d) SLB-$(PLL/PLGA)_4$. The scale bar = 200 μm.

Immunofluorescent Staining of FLSPCs Colonies. FLSPCs colonies were cultured on the series of SLB-PEM substrates and were confirmed as undifferentiated by the expression of their protein profiles. To characterize these colonies biologically, protein expressions were examined for several markers including AFP, CK7, CK19, and DLk. These

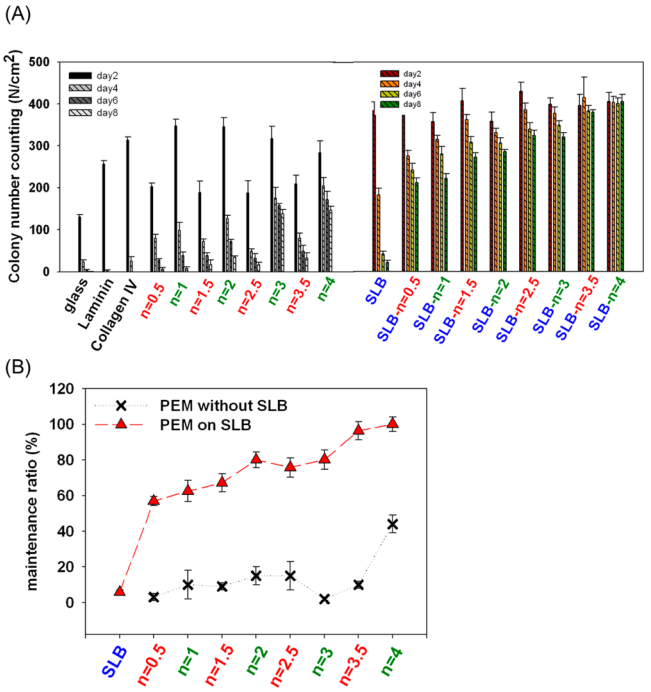

Figure 4. (A) Average numbers of FLSPCs colonies formed on PEM without SLB (gray) and PEM adsorbed on SLB (colored) substrates were calculated on days 2, 4, 6, and 8, respectively. Data show the average of six samples for each coating, with the error bars representing one standard deviation. (B) Maintenance ratio of FLSPCs colonies on PEM without SLB substrates and SLB-PEM substrates.

markers have been found to express undifferentiated FLSPCs and were downregulated upon stem cell differentiation.[47−50] For the FLSPCs on SLB-PEM substrates, almost all of the cells in the colonies exhibited staining after 6 days of culture, as shown in Figure 5. CK19 is expressed in the biliary epithelial cells, hepatoblasts, and AFP, which is characteristic of endoderm. Dlk is a type I membrane that has 6 EGF-like repeats in its extracellular domain and a short cytoplasmic domain.[50,51] Tanimizu et al. revealed that Dlk is strongly expressed in the fetal liver at E10.5.[51] The strong expression continued until the E16.5 stage and significantly downregulated thereafter. Therefore, Dlk was used as a marker to enrich hepatoblasts. Our previous study has revealed that RT-PCR expression is consistent with the expression of immunostaining markers, and it is revealed that these selected colonies displayed positive expression for FLSPCs markers, including Dlk-1, CD49f, CD133, AFP, and ALB. The cytochrome 450 type 3A1 (CYP3A1), a detoxification enzyme expressed by matured hepathocytes, was observed when the induction medium was replaced, and the Dlk marker expression was downregulated after induction.[22] Figure 5 displays the maintenance ability of SLB-PEM substrates; even after 14 days of culture with a medium change, some of the colonies still expressed these proteins and showed an excellent ability to maintain their morphology.

Evaluation of Serum Adsorption Amount on PEM and SLB-PEM Substrates. Because SLB-based PEM substrates exhibited superior selection and maintenance ability compared to the PEM-only substrates, we hypothesized that their nonfouling characteristics and resistance of nonspecific binding of SLB were crucial. To evaluate our hypothesis, we examined

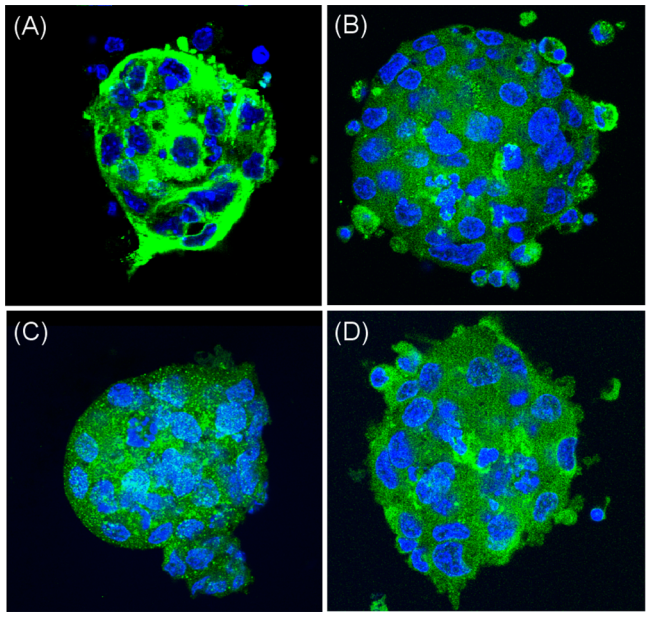

Figure 5. Fluorescent confocal microscopic images of immunofluorescent staining of FLSPC spheroids isolated from SLB-$(PLL/PLGA)_4$ after 6 days of culture. The FLSPCs spheroids were stained with (A) Dlk-1, (B) AFP, (C) CK7, and (D) CK19. Green fluorescence represents immunocytologically positive cells. Blue fluorescence indicated cell nuclei stained by DAPI.

the physicochemical and protein adsorption characteristics of the SLB-PEM films and PEM films. QCM-D analysis was used to monitor serum adsorption. Figure 6 shows the evaluation of

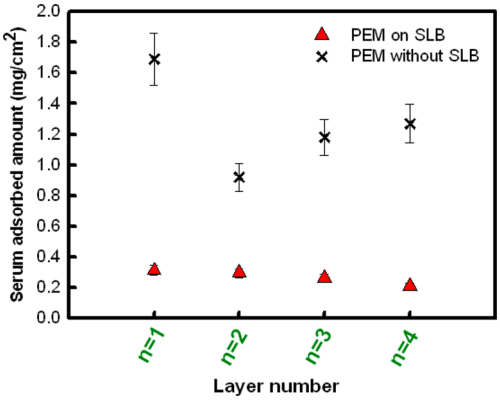

Figure 6. Comparison of the serum adsorption amount on PEM and SLB-PEM systems having a PLL terminal layer, as determined by QCM-D analysis. The amount of adsorbed serum on each film was fitted with the Voigt model.

serum adsorption amount on PEM and the SLB-PEM system with a PLL terminal layer by using Q tool software, because the serum adsorption amount on substrates with a PLL terminal layer is larger than that on substrates with a PLGA terminal layer. Significant, irreversible adsorption was observed in the PEM system, whereas little irreversible adsorption was observed in the SLB-PEM system. Irreversible adsorption was determined on the basis of the serum adsorption amount measured on the surface after 3 rinses with PBS. These results suggest that, when cells do not find adsorbed proteins on the surface on which to bind or do not release adhesion proteins to attach to the surface or create binding sites, colonies would not

attach tightly and cells would not migrate from the colonies. The low levels of adsorption amount to SLB-based surface (0.21−0.32 ng/cm^2) in the serum-containing medium showed the protein-resistant properties of the SLB-PEM substrates. The serum adsorption amounts on PEM substrates were 3.3−5.6 times that of SLB-PEM substrates. We believe that the reduced serum protein adsorption is the main reason for the limitation of colony cell expansion and migration on the SLB-based PEM substrates. However, cells migrated from the colonies on the SLB-only substrate and SLB-PEM substrates having lower number of PEM film layers. This suggests that the SLB structure may be destroyed and result in the appearance of defect sites after long-term culture. Furthermore, those SLB-PEM substrates with a larger number of PEM layers may provide a protecting layer to maintain the composite structure and to avoid the rupture of the underlying SLB.

Evaluation of the Diameter of Cluster. To determine the relationship between colony size and maintenance ratio, the percentage of FLSPC clusters that fell into one of four different cluster diameter categories was analyzed for a range of SLB-PEM substrates after both a 2 and 8 day culture, as shown in the histogram in Figure 7. The diameters of the clusters increased greatly after 8 days on the SLB substrate, which was consistent with the maintenance ratio results shown in Figure 4B. Additionally, the percentage of colonies with diameter up to 50 μm on SLB-PLL also increased after 8 days of culture, suggesting that the clusters spontaneously spread out and changed their morphology into large, flattened or nonregular shapes. In contrast, for SLB-(PLL/PLGA)$_n$, when $n \geq 2.5$, most of the cluster diameters were maintained under 40 μm.

Evaluation of Colony−Materials Interaction. Cells bind to substrates via adhesion molecules, whose intracellular domains are connected to the cytoskeleton. Without binding to the cytoskeleton, a cell adhesion molecule could be hydrolyzed and separated from the cellular membrane. We used vinculin, a cell adhesion molecule, to analyze cell−substrate interaction. Figure 8a−c,d−f shows the vinculin expression of FLSPCs on three types of substrates, c-PLL, SLB-PLL, and SLB-(PLL/PLGA)$_4$ after 4 and 8 days of culture, respectively. Additionally, the high vinculin expression of FLSPCs on SLB only substrate after 8 days culture is shown in Figure 8g. (The culture duration was limited to 8 days because, after more than 8 days, the SLB appeared to rupture, perhaps because it was only 5 nm thick.) The extended phenotypes on vinculin expression were displayed on each of the cells, and the vinculin expression was upregulated as the PEM layer number n increased for the PEM substrates not conjugated with SLB. In contrast, there was only light vinculin expression on SLB-(PLL/PLGA)$_4$ substrates, even after 8 days of culture, which indicates a weak interaction between the FLSPCs colony and the underlying SLB-PEM substrate.

The vinculin expression results demonstrate that the interaction of the colonies with the substrate is affected by the underlying materials, the presence of proteins, and the number of PEM film layers. Richert et al. revealed that the adhesion force decreases when the PEM film thickness increases, which is confirmed by our results.[9] This phenomenon was enhanced in the SLB-based system that we present in this work. In addition, the vinculin expression level results agreed with the cluster size distribution data, offering further proof that the cell−materials interaction decreases as the PEM layer number increases. The decrease in the cell−materials interaction leads, in turn, to an improvement in the maintenance of the cluster size.

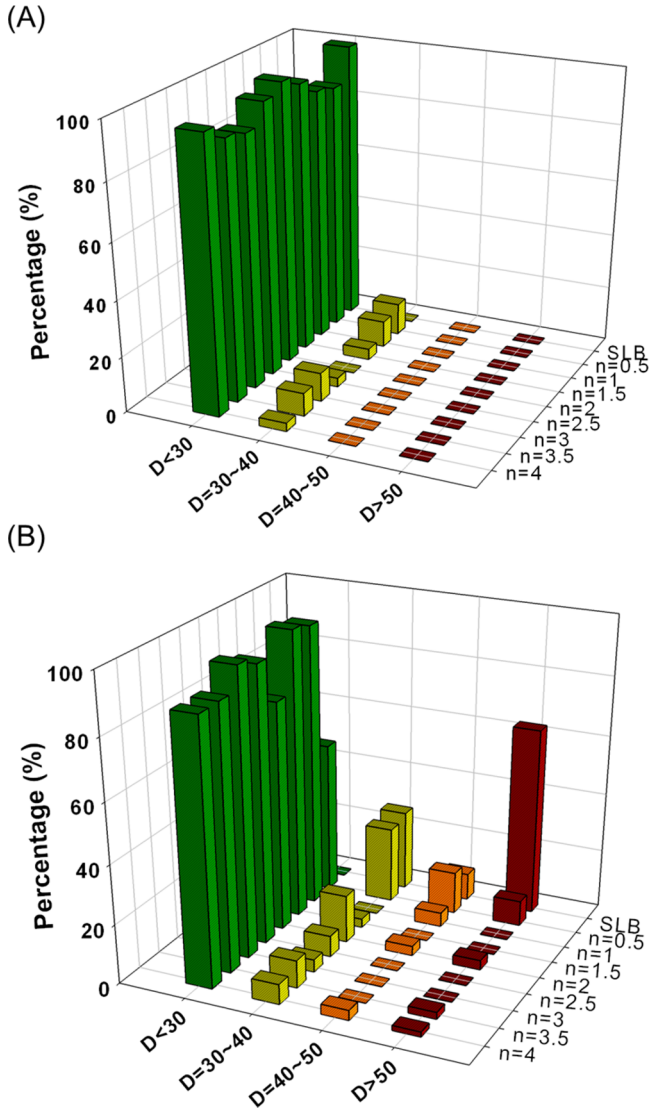

Figure 7. Percentage of populations of FLSPC clusters as a function of cluster diameter, on a series of SLB-PEM substrates after (A) 2 days of culture and (B) 8 days of culture.

DISCUSSION

Purification of stem cells needs to avoid artifacts introduced by *in vitro* manipulation. Stem cell selection from tissues is based on finding a number of morphological and molecular traits, including surface antigens that distinguish them from other cells in the tissue of interest. Until recently, most FLSPCs selection protocols have relied on FACS or magnetic immunosorting and use sets of antibodies against cell surface proteins.[49,51−53] However, there are many complications that accompany the use of FACS isolation, such as its complex procedure and the need to remove surface antigens after cell isolation. Moreover, the survival ratio of the isolated cells acquired via the FACS method is a fundamental question. In addition, when the molecular signature of a particular stem cell is unknown, the task of isolating the stem cells involves a tedious process of screening large numbers of putative markers

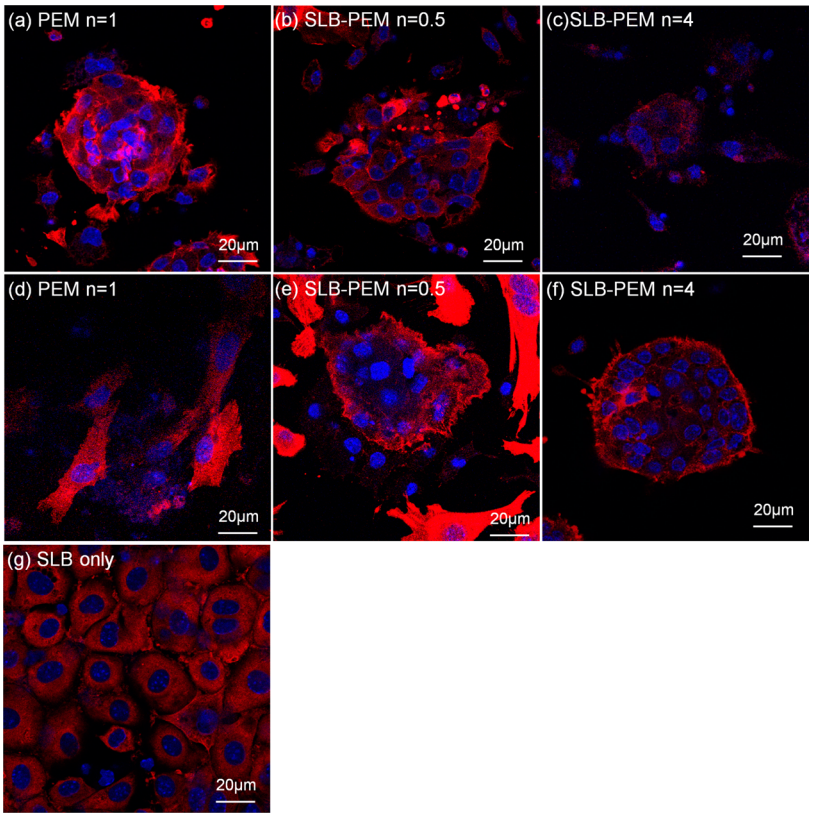

Figure 8. Vinculin expression on the substrates including PEM and SLB-PEM films after 4 and 8 days of culture. (a), (b), and (c) show the down layer of the c-PLL, SLB-PLL, and SLB-$(PLL/PLGA)_4$ after 4 days of culture. (d), (e), (f), and (g) show the down layer of the c-PLL, SLB-PLL, SLB-$(PLL/PLGA)_4$, and SLB only after 8 days of culture.

to identify the ones that cosegregate with functional attributes of stemness.

As an initial step toward the application of FLSPCs to tissue engineering, a simple, rapid, label-free method of stem cell colony selection and maintenance was established in the work presented here. This semiattached selection and culture system has the advantage that it limits cell anchorage and matrix remolding, two effects that can result in spontaneous stem cell differentiation and mechanical damage. In the case of SLB-PEM substrates in this work, the surface properties maintain the specialized features of cultured cells.

Another factor that increases the difficulty inherent in the isolation and maintenance of specific cells arises from the necessity of serum protein for stem cell colony formation; the adsorption of the serum, however, can interfere with the cell–materials interaction and may result in the stem cell differentiation. As indicated in our previous study, serum is a crucial factor on colony formation in this system.[22] However, serum adsorption resulted in spontaneous differentiation of the stem cells. The balance of the two effects is a key issue in this study. In previous work, we demonstrated that the PEM films have a better maintenance ratio when they had four complete layers (n = 4); however, the maintenance ratio was not satisfactory. In this work, we introduced a protein-repellent material, SLB, into the system to enhance the maintenance ratio of the PEM-only system. An SLB-based system is an ideal candidate for providing the fluidity of biologic membranes that borders all cells in the human body. Proteins and lipids are the key building blocks of biomembranes. The lipids form a continuous, essentially two-dimensional, phase into which the functional proteins are discretely incorporated. The previous literature has observed that, for some of the polymer surfaces, after being treated with different types of lipid bilayers, the protein adsorption was further reduced.[54,55] The suggestion is that the nonfouling properties of SLB may be related to many aspects including the fluid versus nonfluid properties resulting in the viscoelastic properties of the surface or the water interaction and polarizability of the SLB. These properties result in the different domains of the SLB surface. Our results reveal that we generate large number of stem cell colonies, as well as maintain them on the surfaces after long-term culture regardless of its rigidity. We suggest that a protein adsorption-free surface has prevented cell spreading as well as differentiation. It is noted that the colonies cannot be maintained on a pure SLB substrate, suggesting that the PEM may provide a protection layer to prevent the SLB breakage. Glasmastar et al. have also used QCM-D to determine the adsorbed property of PC lipid and revealed that about 70 times more mass is adsorbed on a TiO_2 surface than on a phospholipid bilayer.[42] They also investigated the adsorption with other proteins including fibrinogen, human serum albumin, and bovine hemoglobin under similar conditions. As cell membranes carry negative charges in physiological conditions, the substrate with a terminal layer with a negative charge of PLGA displayed better colony formation and maintenance ratio. In addition, the terminal layer effect decreased as the number of layers increased. This further suggests that the reduction of the adhesion force with increasing film thickness may be due to the variation of the external structure of the multilayer and may influence the protein adsorption. However, using SLB as the base substrate can provide a biomimetic system and fabricate a stem cell environment that resists protein adsorption without

the terminal layer effect. Furthermore, it is considered that the PEM conjugation on SLB substrate can further strengthen the SLB structure that resulted in the increase of the maintenance ratio as the number of PEM layers increased.

CONCLUSIONS

In our previous work, we have shown that the FLSPCs selectively adhere and form colonies on PLL/PLGA PEM films. In this study, we used SLBs as the base materials to modify the biomimetic substrate and provide a series of surface environment variations. We have shown that FLSPCs also form colonies on SLB-PEM substrates and the stem cell selection ratio is unrelated to the terminal layer of the PEM. In addition, the maintenance ratio was greater on all of the SLB-PEM substrates compared to PEM-only substrates. Significantly, the maintenance ratio increased to ~100% on SLB-$(PLL/PLGA)_4$ films. The SLB-based films provide nonfouling and nonstick properties to prevent protein adsorption and stem cell anchorage, which created a new insight beyond environmental selection based on stiffness. Furthermore, in comparison to PEM-only films, the SLB-PEM system provides important information on the cell−cell and cell−materials interactions. We believe this material provides a novel platform and a new option for stem cell research that can facilitate liver stem cells use and can even be applied to other kinds of stem cell selections.

ASSOCIATED CONTENT

Supporting Information

Figure S1, AFM images of SLB-PEM films on mica. Figure S2, the FRAP experiment of quantitative traces of the fluorescence intensity across the bleached spot after 30 min and the relative diffusion coefficients. This material is available free of charge via the Internet at http://pubs.acs.org.

AUTHOR INFORMATION

Corresponding Author

*Phone: +886 2 27871277. Fax: +886 2 27899931. E-mail: yingchih@gate.sinica.edu.tw.

Present Address

[§]H.-A.T.: No. 28, Hua Dong Road, Daliao District, Kaohsiung City 83162, SeeCURE, Taiwan.

Notes

The authors declare no competing financial interest.

ACKNOWLEDGMENTS

We would like to thank the financial support obtained from National Science Council, Taiwan 101-2113-M-001-021-MY2 (2011-2013), and Summit Project, Academic Sinica. I-C. Lee was also supported by Chang-Gung University and Chang Gung Hospital Grants: CMRPD1A0061 and CMRPD1A0062.

REFERENCES

(1) Lutolf, M. P.; Blau, H. M. Artificial Stem Cell Niches. *Adv. Mater.* **2009**, *21*, 3255−3268.

(2) Hosseinkhani, M.; Shirazi, R.; Rajaei, F.; Mahmoudi, M.; Mohammadi, N.; Abbasi, M. Engineering of the Embryonic and Adult Stem Cell Niches. *Iran. Red Crescent Med. J.* **2013**, *15*, 83−92.

(3) Conway, A.; Schaffer, D. V. Biophysical Regulation of Stem Cell Behavior within the Niche. *Stem Cell Res. Ther.* **2012**, *3*, 50.

(4) Cha, C.; Liechty, W. B.; Khademhosseini, A.; Peppas, N. A. Designing Biomaterials to Direct Stem Cell Fate. *ACS Nano* **2012**, *6*, 9353−9358.

(5) Pierini, M.; Dozza, B.; Lucarelli, E.; Tazzari, P. L.; Ricci, F.; Remondini, D.; di Bella, C.; Giannini, S.; Donati, D. Efficient Isolation and Enrichment of Mesenchymal Stem Cells from Bone Marrow. *Cytotherapy* **2012**, *14*, 686−693.

(6) Zhang, L.; Chan, C. Isolation and Enrichment of Rat Mesenchymal Stem Cells (MSCs) and Separation of Single-Colony Derived MSCs. *J. Visualized Exp.* **2010**, DOI: 10.3791/1852.

(7) Huang, X.; Ketova, T.; Litingtung, Y.; Chiang, C. Isolation, Enrichment, and Maintenance of Medulloblastoma Stem Cells. *J. Visualized Exp.* **2010**, DOI: 10.3791/2086.

(8) Bosio, A.; Huppert, V.; Donath, S.; Hennemann, P.; Malchow, M.; Heinlein, U. A. Isolation and Enrichment of Stem Cells. *Adv. Biochem. Eng./Biotechnol.* **2009**, *114*, 23−72.

(9) Richert, L.; Lavalle, P.; Vautier, D.; Senger, B.; Stoltz, J. F.; Schaaf, P.; Voegel, J. C.; Picart, C. Cell Interactions with Polyelectrolyte Multilayer Films. *Biomacromolecules* **2002**, *3*, 1170−1178.

(10) Etienne, O.; Gasnier, C.; Taddei, C.; Voegel, J. C.; Aunis, D.; Schaaf, P.; Metz-Boutigue, M. H.; Bolcato-Bellemin, A. L.; Egles, C. Antifungal Coating by Biofunctionalized Polyelectrolyte Multilayered Films. *Biomaterials* **2005**, *26*, 6704−6712.

(11) Decher, G.; Hong, J. D. In Buildup of Ultrathin Multilayer Films by a Self-Assembly Process: 2. Consecutive Adsorption of Anionic and Cationic Bipolar Amphiphiles and Polyelectrolytes on Charged Surfaces. *Ber. Bunsen-Ges. Phys. Chem.* **1991**, *95*, 1430−1434.

(12) Boura, C.; Muller, S.; Vautier, D.; Dumas, D.; Schaaf, P.; Claude Voegel, J.; Francois Stoltz, J.; Menu, P. Endothelial Cell–Interactions with Polyelectrolyte Multilayer Films. *Biomaterials* **2005**, *26*, 4568−4575.

(13) Brunot, C.; Ponsonnet, L.; Lagneau, C.; Farge, P.; Picart, C.; Grosgogeat, B. Cytotoxicity of Polyethyleneimine (PEI), Precursor Base Layer of Polyelectrolyte Multilayer Films. *Biomaterials* **2007**, *28*, 632−640.

(14) Daubine, F.; Cortial, D.; Ladam, G.; Atmani, H.; Haikel, Y.; Voegel, J. C.; Clezardin, P.; Benkirane-Jessel, N. Nanostructured Polyelectrolyte Multilayer Drug Delivery Systems for Bone Metastasis Prevention. *Biomaterials* **2009**, *30*, 6367−6373.

(15) Kurihara, K. Polyelectrolyte Brushes Studied by Surface Forces Measurement. *Adv. Colloid Interface Sci.* **2010**, *158*, 130−138.

(16) Croll, T. I.; O'Connor, A. J.; Stevens, G. W.; Cooper-White, J. J. A Blank Slate? Layer-by-Layer Deposition of Hyaluronic Acid and Chitosan onto Various Surfaces. *Biomacromolecules* **2006**, *7*, 1610−1622.

(17) Hajicharalambous, C. S.; Lichter, J.; Hix, W. T.; Swierczewska, M.; Rubner, M. F.; Rajagopalan, P. Nano- and Sub-Micron Porous Polyelectrolyte Multilayer Assemblies: Biomimetic Surfaces for Human Corneal Epithelial Cells. *Biomaterials* **2009**, *30*, 4029−4036.

(18) Samuel, R. E.; Shukla, A.; Paik, D. H.; Wang, M. X.; Fang, J. C.; Schmidt, D. J.; Hammond, P. T. Osteoconductive Protamine-Based Polyelectrolyte Multilayer Functionalized Surfaces. *Biomaterials* **2011**, *32*, 7491−7502.

(19) Yamanlar, S.; Sant, S.; Boudou, T.; Picart, C.; Khademhosseini, A. Surface Functionalization of Hyaluronic Acid Hydrogels by Polyelectrolyte Multilayer Films. *Biomaterials* **2011**, *32*, 5590−5599.

(20) Grossin, L.; Cortial, D.; Saulnier, B.; Félix, O.; Chassepot, A.; Decher, G.; Netter, P.; Schaaf, P.; Gillet, P.; Mainard, D.; Voegel, J.-C.; Benkirane-Jessel, N. Step-by-Step Build-Up of Biologically Active Cell-Containing Stratified Films Aimed at Tissue Engineering. *Adv. Mater.* **2009**, *21*, 650−655.

(21) Mhamdi, L.; Picart, C.; Lagneau, C.; Othmane, A.; Grosgogeat, B.; Jaffrezic-Renault, N.; Ponsonnet, L. Study of the Polyelectrolyte Multilayer Thin Films' Properties and Correlation with the Behavior of the Human Gingival Fibroblasts. *Mater. Sci. Eng., C* **2006**, *26*, 273−281.

(22) Tsai, H. A.; Wu, R. R.; Lee, I. C.; Chang, H. Y.; Shen, C. N.; Chang, Y. C. Selection, Enrichment, and Maintenance of Self-Renewal Liver Stem/Progenitor Cells Utilizing Polypeptide Polyelectrolyte Multilayer Films. *Biomacromolecules* **2010**, *11*, 994−1001.

(23) Tsai, H. A.; Shen, C. N.; Chang, Y. C. Use of Surface Properties to Control the Growth and Differentiation of Mouse Fetal Liver Stem/Progenitor Cell Colonies. *Biomacromolecules* **2012**, *13*, 3483−3493.
(24) Li, J.; Han, D.; Zhao, Y. P. Kinetic Behaviour of the Cells Touching Substrate: The Interfacial Stiffness Guides Cell Spreading. *Sci. Rep.* **2014**, *4*, 3910.
(25) Discher, D. E.; Janmey, P.; Wang, Y. L. Tissue Cells Feel and Respond to the Stiffness of Their Substrate. *Science* **2005**, *310*, 1139−1143.
(26) Yeung, T.; Georges, P. C.; Flanagan, L. A.; Marg, B.; Ortiz, M.; Funaki, M.; Zahir, N.; Ming, W.; Weaver, V.; Janmey, P. A. Effects of Substrate Stiffness on Cell Morphology, Cytoskeletal Structure, and Adhesion. *Cell Motil. Cytoskeleton* **2005**, *60*, 24−34.
(27) Tan, H.; Gao, X.; Sun, J.; Xiao, C.; Hu, X. Double Stimulus-Induced Stem Cell Aggregation During Differentiation on a Biopolymer Hydrogel Substrate. *Chem. Commun.* **2013**, *49*, 11554−11556.
(28) Bernard, A. B.; Lin, C. C.; Anseth, K. S. A Microwell Cell Culture Platform for the Aggregation of Pancreatic Beta-Cells. *Methods Tissue Eng., Part C* **2012**, *18*, 583−592.
(29) Mohr, J. C.; de Pablo, J. J.; Palecek, S. P. 3-D Microwell Culture of Human Embryonic Stem Cells. *Biomaterials* **2006**, *27*, 6032−6042.
(30) Merian, T.; Goddard, J. M. Advances in Nonfouling Materials: Perspectives for the Food Industry. *J. Agric. Food Chem.* **2012**, *60*, 2943−2957.
(31) Yu, Q.; Zhang, Y.; Wang, H.; Brash, J.; Chen, H. Anti-Fouling Bioactive Surfaces. *Acta Biomater.* **2011**, *7*, 1550−1557.
(32) Phillips, K. S.; Han, J. H.; Cheng, Q. Development of a "Membrane Cloaking" Method for Amperometric Enzyme Immunoassay and Surface Plasmon Resonance Analysis of Proteins in Serum Samples. *Anal. Chem.* **2007**, *79*, 899−907.
(33) Sharma, S.; Desai, T. A. Nanostructured Antifouling Poly(Ethylene Glycol) Films for Silicon-Based Microsystems. *J. Nanosci. Nanotechnol.* **2005**, *5*, 235−243.
(34) Wu, D.; Zhao, B.; Dai, Z.; Qin, J.; Lin, B. Grafting Epoxy-Modified Hydrophilic Polymers onto Poly(Dimethylsiloxane) Microfluidic Chip to Resist Nonspecific Protein Adsorption. *Lab Chip* **2006**, *6*, 942−947.
(35) Patel, S.; Thakar, R. G.; Wong, J.; McLeod, S. D.; Li, S. Control of Cell Adhesion on Poly(Methyl Methacrylate). *Biomaterials* **2006**, *27*, 2890−2897.
(36) Pidhatika, B.; Rodenstein, M.; Chen, Y.; Rakhmatullina, E.; Muhlebach, A.; Acikgoz, C.; Textor, M.; Konradi, R. Comparative Stability Studies of Poly(2-Methyl-2-Oxazoline) and Poly(Ethylene Glycol) Brush Coatings. *Biointerphases* **2012**, *7*, 1.
(37) Liu, Q.; Singh, A.; Lalani, R.; Liu, L. Ultralow Fouling Polyacrylamide on Gold Surfaces via Surface-Initiated Atom Transfer Radical Polymerization. *Biomacromolecules* **2012**, *13*, 1086−1092.
(38) Monchaux, E.; Vermette, P. Development of Dextran-Derivative Arrays to Identify Physicochemical Properties Involved in Biofouling from Serum. *Langmuir* **2007**, *23*, 3290−3297.
(39) Dilly, S. J.; Beecham, M. P.; Brown, S. P.; Griffin, J. M.; Clark, A. J.; Griffin, C. D.; Marshall, J.; Napier, R. M.; Taylor, P. C.; Marsh, A. Novel Tertiary Amine Oxide Surfaces that Resist Nonspecific Protein Adsorption. *Langmuir* **2006**, *22*, 8144−8150.
(40) Sirbuly, D. J.; Fischer, N. O.; Huang, S. C.; Artyukhin, A. B.; Tok, J. B.; Bakajin, O.; Noy, A. Biofunctional Subwavelength Optical Waveguides for Biodetection. *ACS Nano* **2008**, *2*, 255−262.
(41) Marsh, D.; Bartucci, R.; Sportelli, L. Lipid Membranes with Grafted Polymers: Physicochemical Aspects. *Biochim. Biophys. Acta* **2003**, *1615*, 33−59.
(42) Glasmastar, K.; Larsson, C.; Hook, F.; Kasemo, B. Protein Adsorption on Supported Phospholipid Bilayers. *J. Colloid Interface Sci.* **2002**, *246*, 40−47.
(43) Ho, J. A.; Kuo, T. Y.; Yu, L. G. Dual Polarization Interferometric and Capillary Electrophoretic Analysis of Supported Lipid Bilayer Constructed on Silica-Based Surface: Evaluation of its Anti-Protein Adsorption Effect. *Anal. Chim. Acta* **2012**, *714*, 127−133.
(44) Huang, C. J.; Cho, N. J.; Hsu, C. J.; Tseng, P. Y.; Frank, C. W.; Chang, Y. C. Type I Collagen-Functionalized Supported Lipid Bilayer as a Cell Culture Platform. *Biomacromolecules* **2010**, *11*, 1231−1240.
(45) Höök, F.; Vörös, J.; Rodahl, M.; Kurrat, R.; Böni, P.; Ramsden, J. J.; Textor, M.; Spencer, N. D.; Tengvall, P.; Gold, J.; Kasemo, B. A Comparative Study of Protein Adsorption on Titanium Oxide Surfaces Using in Situ Ellipsometry, Optical Waveguide Lightmode Spectroscopy, and Quartz Crystal Microbalance/Dissipation. *Colloids Surf., B* **2002**, *24*, 155−170.
(46) Lee, I. C.; Wu, Y. C. Facilitating Neural Stem/Progenitor Cell Niche Calibration for Neural Lineage Differentiation by Polyelectrolyte Multilayer Films. *Colloids Surf., B* **2014**, *121*, 54−65.
(47) Kakinuma, S.; Ohta, H.; Kamiya, A.; Yamazaki, Y.; Oikawa, T.; Okada, K.; Nakauchi, H. Analyses of Cell Surface Molecules on Hepatic Stem/Progenitor Cells in Mouse Fetal Liver. *J. Hepatol.* **2009**, *51*, 127−138.
(48) Zhou, H.; Rogler, L. E.; Teperman, L.; Morgan, G.; Rogler, C. E. Identification of Hepatocytic and Bile Ductular Cell Lineages and Candidate Stem Cells in Bipolar Ductular Reactions in Cirrhotic Human Liver. *Hepatology* **2007**, *45*, 716−724.
(49) Herrera, M. B.; Bruno, S.; Buttiglieri, S.; Tetta, C.; Gatti, S.; Deregibus, M. C.; Bussolati, B.; Camussi, G. Isolation and Characterization of a Stem Cell Population from Adult Human Liver. *Stem Cells* **2006**, *24*, 2840−2850.
(50) Tanimizu, N.; Tsujimura, T.; Takahide, K.; Kodama, T.; Nakamura, K.; Miyajima, A. Expression of Dlk/Pref-1 Defines a Subpopulation in the Oval Cell Compartment of Rat Liver. *Gene Expression Patterns* **2004**, *5*, 209−218.
(51) Tanimizu, N.; Nishikawa, M.; Saito, H.; Tsujimura, T.; Miyajima, A. Isolation of Hepatoblasts Based on the Expression of Dlk/Pref-1. *J. Cell Sci.* **2003**, *116*, 1775−1786.
(52) Yanai, H.; Nakamura, K.; Hijioka, S.; Kamei, A.; Ikari, T.; Ishikawa, Y.; Shinozaki, E.; Mizunuma, N.; Hatake, K.; Miyajima, A. Dlk-1, a Cell Surface Antigen on Foetal Hepatic Stem/Progenitor Cells, is Expressed in Hepatocellular, Colon, Pancreas and Breast Carcinomas at a High Frequency. *J. Biochem.* **2010**, *148*, 85−92.
(53) Conigliaro, A.; Colletti, M.; Cicchini, C.; Guerra, M. T.; Manfredini, R.; Zini, R.; Bordoni, V.; Siepi, F.; Leopizzi, M.; Tripodi, M.; Amicone, L. Isolation and Characterization of a Murine Resident Liver Stem Cell. *Cell Death Differ.* **2008**, *15*, 123−133.
(54) Kim, H. K.; Kim, K.; Byun, Y. Preparation of a Chemically Anchored Phospholipid Monolayer on an Acrylated Polymer Substrate. *Biomaterials* **2005**, *26*, 3435−3444.
(55) Kaladhar, K.; Sharma, C. P. Supported Cell Mimetic Monolayers and Their Interaction with Blood. *Langmuir* **2004**, *20*, 11115−11122.